ARTICLE

Check for updates

Trends in the atmospheric jet streams are emerging in observations and could be linked to tropical warming

Tim Woollings [1✉], Marie Drouard[2], Christopher H. O'Reilly [3], David M. H. Sexton[4] & Carol McSweeney[4]

Climate models predict a weak poleward shift of the jets in response to continuing climate change. Here we revisit observed jet trends using 40 years of satellite-era reanalysis products and find evidence that general poleward shifts are emerging. The significance of these trends is often low and varies between datasets, but the similarity across different seasons and hemispheres is notable. While much recent work has focused on the jet response to amplified Arctic warming, the observed trends are more consistent with the known sensitivity of the circulation to tropical warming. The circulation trends are within the range of historical model simulations but are relatively large compared to the models when the accompanying trends in upper tropospheric temperature gradients are considered. The balance between tropical warming and jet shifts should therefore be closely monitored in the near future. We hypothesise that the sensitivity of the circulation to tropical heating may be one factor affecting this balance.

[1] Atmospheric, Oceanic and Planetary Physics, University of Oxford, OX1 3PU Oxford, UK. [2] Instituto de Geociencias (IGEO), CSIC-UCM, Madrid, Spain. [3] Department of Meteorology, University of Reading, Reading, UK. [4] Met Office Hadley Centre, FitzRoy Road, Exeter EX1 3PB, UK. ✉email: tim.woollings@physics.ox.ac.uk

Jet streams comprise strong zonal wind belts which form on rotating planets in response to stirring of the atmosphere due to instabilities related to meridional density contrasts. As such, Earth's jet streams are sensitive to the equator to pole temperature contrasts in the strength of anthropogenic warming[1]. While a diverse array of physical processes can affect the jets, including cloud cover[2] and stratospheric flow[3], the two leading ingredients are the contrasting changes to temperature gradients in the upper and lower troposphere.

Much attention has recently focused on the amplified warming of the Arctic, which weakens the meridional temperature gradient in the lower troposphere[4]. In isolation, this is widely predicted to shift the northern hemisphere jet stream equatorwards, in particular by weakening the baroclinicity on the poleward flank of the associated storm tracks[5,6]. In the upper troposphere, however, predicted warming is strongest in the tropics and hence a competing effect acts to push the jets poleward instead[7,8]. The opposition of these two effects leads to a relatively small projected poleward shift of the jet in response to tropical warming, which is partially offset by the effects of Arctic amplification[9–13].

Despite the apparent dominance of tropical forcing in model projections, confidence in these projections has been limited by uncertainty over the strength of tropical warming[14]. The amplified Arctic warming is a striking feature of observed trends, associated with a range of processes including poleward heat transport and local feedbacks[15]. The enhancement of warming in the tropical upper troposphere is expected as a consequence of the moist adiabatic structure of the tropical atmosphere, but in contrast to the Arctic there remains uncertainty over its

strength[16], with some observational estimates remaining weaker than the warming in model simulations[17].

Since model circulation responses are weak, present-day jet behaviour might be expected to be dominated by natural variability[18], with the exception of the strong southern hemisphere summertime jet shift associated with stratospheric ozone loss[19]. Some studies have detected weak signals associated with poleward jet shifts in observed data[20] but the patterns of change have so far appeared complex and regional[21]. In this paper, we revisit the observed jet trends using the latest reanalyses and attempt to reconcile these with the apparently weak warming of the tropical upper troposphere. Trends in reanalysis data should always be treated with caution[22], but the emergence of related trends in pressure and cloud observations offers some support[23,24].

Results

Figure 1a shows the linear trend of December–February (DJF) zonal mean zonal wind over the period of satellite observations using the ERA5 reanalysis. The structure of these trends reflects clear poleward shifts of the main westerly jet streams in both hemispheres, as well as an additional weakening of the westerlies in high northern latitudes. All of these features are deep, equivalent barotropic structures characteristic of the effects of transient eddy forcing[25]. Also apparent is an upwards extension of the jets associated with the lifting of the tropopause. The structure of these trends is clearer in contrast to previous assessments using shorter time periods or more regional methods, especially in the northern hemisphere[20,21]. There is
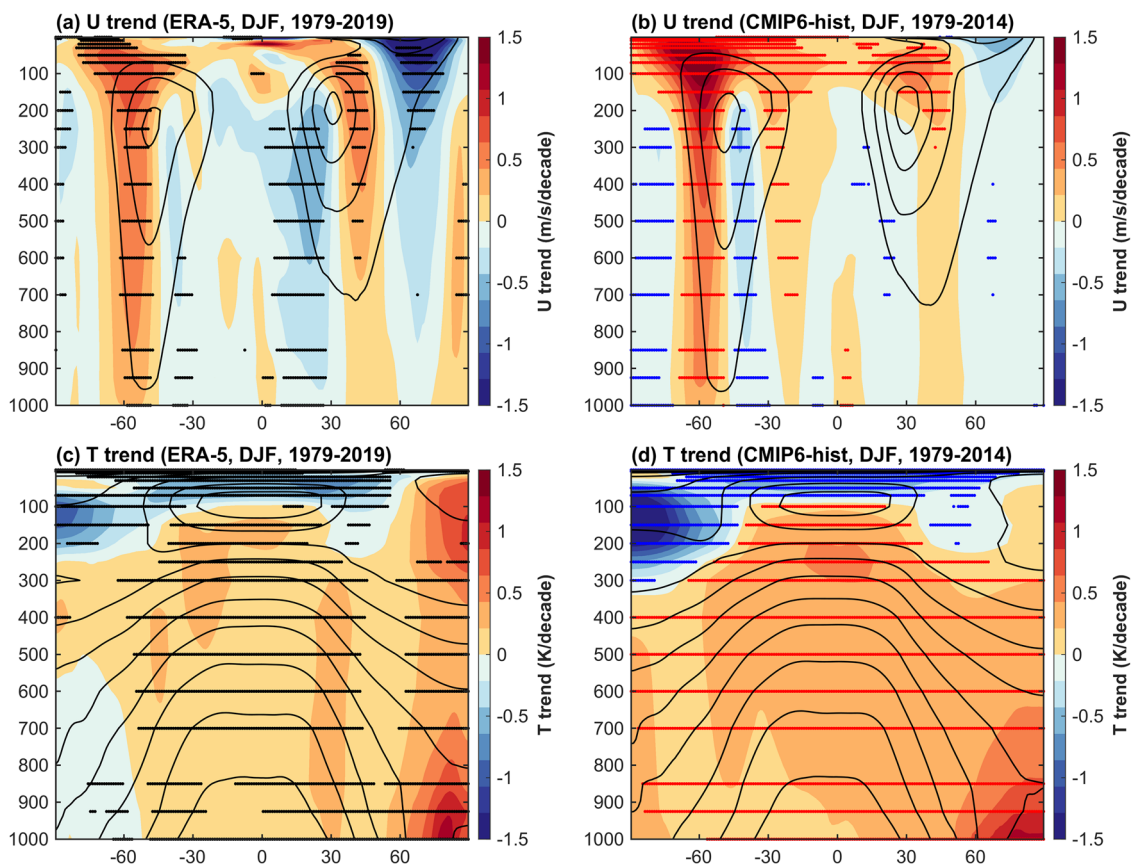

Fig. 1 Linear trends in DJF zonal mean zonal wind and temperature as a function of latitude and pressure from ERA5 and the CMIP6 historical simulations. (**a**) and (**c**) show the wind and temperature respectively from ERA5, and (**b**) and (**d**) show the same for CMIP6. Black dots in the ERA5 panels indicate significance at the 5% level using a T-test. Red and blue dots in the CMIP6 panels indicate that 75% of models agree on the sign of the trend, positive or negative, respectively. Solid lines mark the climatologies with intervals of 10 m s^{-1} and 10K.

some evidence of pointwise statistical significance of these trends but the significance level is sensitive to the choice of method.

A clearer assessment of the significance is given in Fig. 2, which uses the well-established method of zonal indices to measure the jet shifts. Latitude bands spanning the time mean jet maxima are chosen to calculate these zonal indices. This approach avoids multiple testing issues and also allows a comparison across a range of state-of-the-art reanalyses. The only case with clear significance on its own is the southern hemisphere in DJF (Fig. 2b), when ozone forcing is known to play a role. Positive zonal index trends corresponding to poleward shifts are ubiquitous in the other cases shown, though the significance varies between reanalyses. ERA5 shows positive trends in the northern hemisphere DJF ($p = 0.035$) and southern hemisphere June–August (JJA; $p = 0.059$) cases, but the trends in other reanalyses are less significant. The recent observational record clearly remains an uncomfortably short period over which to have confidence in trends in the highly variable circulation, but the consistency of the poleward jet shifts found here is notable. If different regions are combined, as in Fig. 2c, the trends are highly significant. Other seasons show weaker trends although some evidence of a poleward shift is apparent in all cases, with weakening of subtropical winds being of particular significance (Supplementary Fig. 1). Overall, the reanalyses suggest that poleward jet shifts are emerging in the recent historical period at a global scale. Comparison with the previous modelling studies described above suggests that this change is consistent with the dominant influence of tropical warming on the jet streams, as opposed to the effects of Arctic warming.

Returning to the structure of trends, Fig. 1b shows ensemble mean linear wind trends from the CMIP6 historical climate model simulations over a similar period, for comparison with the reanalysis. These model trends show a very similar structure to the observed changes, including a lifting and poleward shift of the jets. This similarity suggests that anthropogenic forcing, as imposed in the historical simulations, may have made an important contribution to the observed jet changes. Other model experiments suggest that stratospheric ozone depletion had a strong contribution to the southern hemisphere linear trends over this period, despite the recent partial recovery of ozone[26], and this is where both model and observed trends are clearest. The southern hemisphere trends appear stronger in the models, and the northern hemisphere trends appear stronger in the observations, but the ensemble mean may be misleading in this regard.

Natural decadal variability may also have played a role in the observed trends, noting that such variability is often underestimated by climate models[27]. Variations associated with the Pacific Decadal Oscillation (PDO) could contribute to the trends shown here[28], although a linear regression analysis suggests this contribution is only minor (Supplementary Fig. 2a). Atlantic Multidecadal Variability (AMV) exhibits a larger trend over this period, and so has potential to play a more significant role. Attempting to remove the AMV signal using linear regression does affect the trends significantly (Supplementary Fig. 2b), however, this likely reflects the collinearity of AMV with the climate change signal during this period, rather than a causal influence. Indeed, the horizontal structure of the linear trends shows signals which are strongest over the Asian continent and the Pacific (Supplementary Fig. 3). This suggests that Atlantic
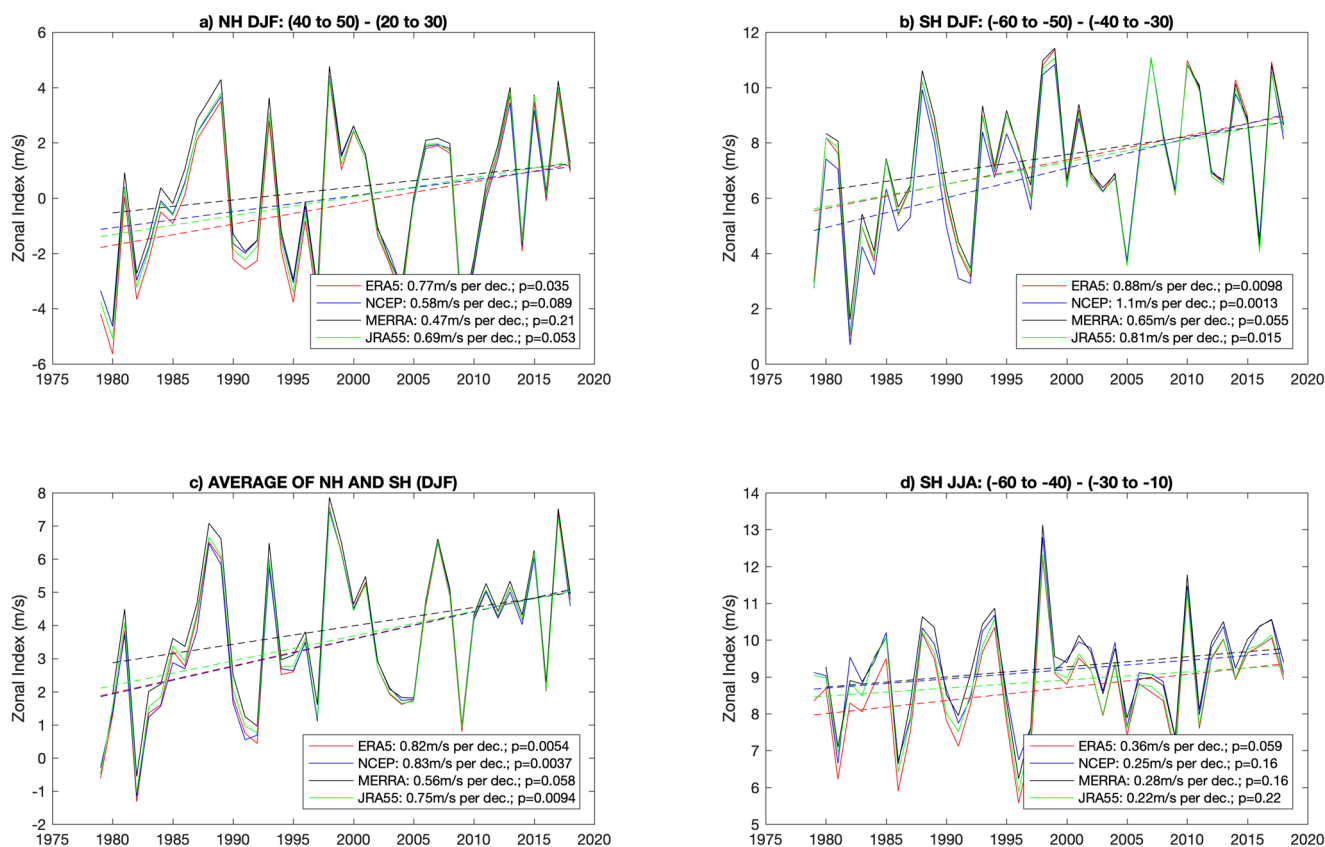

Fig. 2 Zonal indices summarising the wind trends at 500 hPa in four reanalyses: ERA5, NCEP- NCAR, MERRA2, and JRA55. Each index is formed by taking the difference of the zonal mean zonal wind over the two latitude bands given in the title of each subplot. Best fit linear trend lines are shown dashed, with the slopes and p-values (according to a T-test) shown in the legend. Panel (**c**) is the sum of panels (**a**) Northern Hemisphere and (**b**) Southern Hemisphere, and hence provides a global picture for DJF. Panel (**d**) is for Southern Hemisphere JJA.

sector variability does not dominate the zonal mean trends, potentially consistent with observed trends in wind speed and shear in this sector as opposed to jet position[29,30]. Figure 1c, d shows zonal mean temperature trends from both ERA5 and CMIP6. As previously mentioned, tropospheric temperature trends vary considerably between observational datasets. Here we choose to focus on reanalysis trends for dynamical consistency with the wind trends[31]. Intriguingly, the warming in the tropical upper troposphere is markedly stronger in the model simulations than the reanalysis. This is consistent with the relatively strong near-surface warming also seen in Fig. 1d, a known feature of CMIP6 historical simulations over this period[32]. The emergence of observed poleward jet shifts despite relatively weak tropical warming motivates a deeper comparison of the observed and modelled changes.

To quantify these changes better, in Fig. 3 we use zonal indices to summarise the wind trends and compare these to changes in the upper tropospheric temperature gradients. Note that the temperature gradients are focused on regional bands of latitude centred on the time mean jets, rather than from equator to pole as in some studies[9]. CMIP6 historical simulations are used to generate the two-dimensional histograms, and we also show the twenty perturbed physics HadGEM3 ensemble members of the UKCP project, termed UKCP-PPE20 here. The northern hemisphere winter case is shown in Fig. 3a, with the temperature and

wind trends from four different reanalyses marked with crosses. The model trends show considerable spread, with wind trends of both signs and a range of largely strengthening temperature gradients. For the wind trends in particular, it is important to note that the observed trends are not outside the range of the CMIP6 ensemble. However, they are notable for showing a relatively strong trend in the winds given a relatively weak trend in the temperature gradient, consistent with the impression given by Fig. 1. Figure 3b shows the corresponding analysis for southern summer; again the observations exhibit a relatively large circulation trend given the trend in temperature gradient, and are on the edge of the model distribution. The models in this case show a clear correlation between wind and temperature gradients, which is not apparent in the northern winter case. This may reflect the stronger forced component of change in the models' southern hemisphere jets as a result of anthropogenic ozone trends, indicating by comparison that much of the spread in panel (a) is likely due to natural variability. In the June-August (JJA) season the reanalyses similarly show weak trends in temperature gradient and positive trends in zonal index in the southern hemisphere (Fig. 3d), while the northern case shows generally weak trends (Fig. 3c).

In summary, observed poleward jet shifts are apparent in several cases, with northern hemisphere JJA being distinct in showing no evidence of a poleward shift (Supplementary Fig. 1).
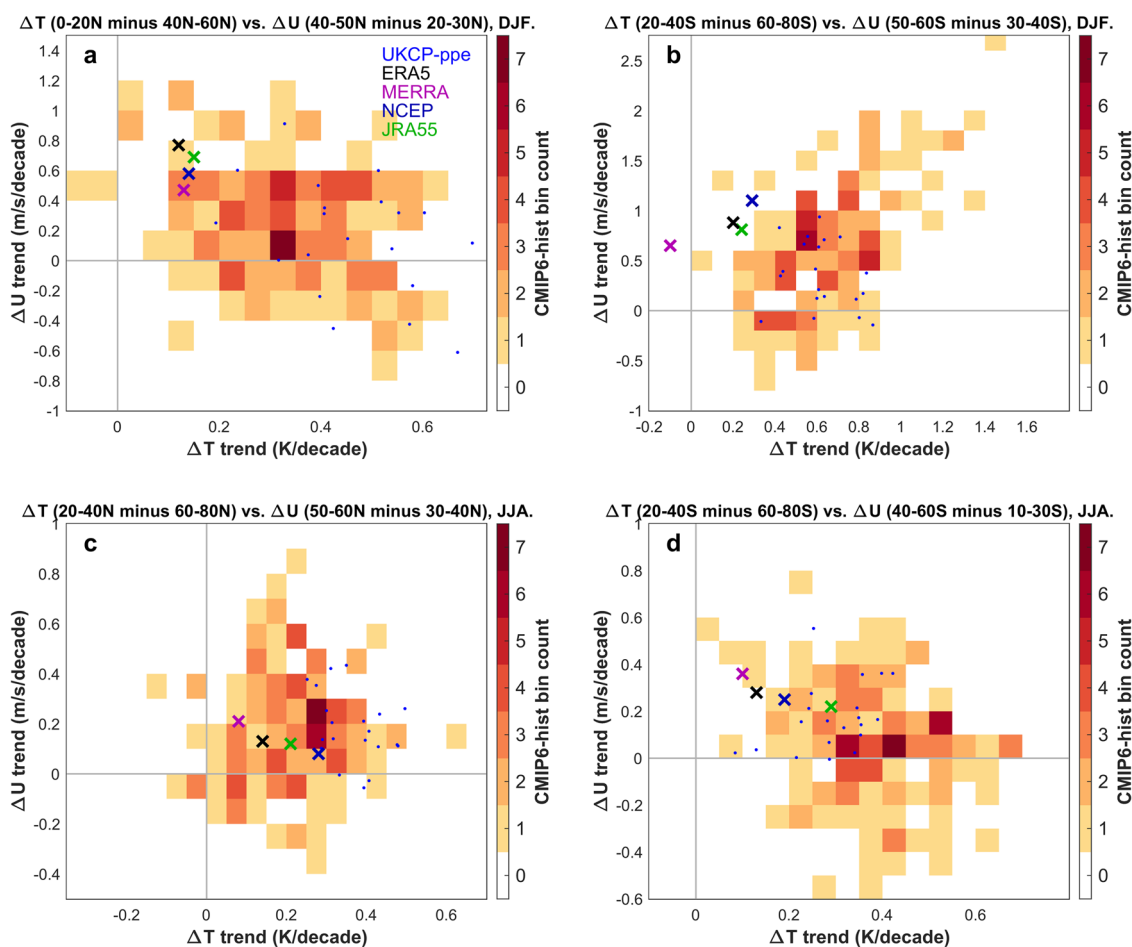

Fig. 3 Trends in 500hPa zonal wind indices plotted against the trends in 250hPa meridional temperature gradient. (**a**) Northern hemisphere DJF; (**b**) Southern hemisphere DJF; (**c**) Northern hemisphere JJA; (**d**) Southern hemisphere JJA. The zonal wind indices are calculated by subtracting the mean zonal wind at high latitudes from the wind at low latitudes. In contrast the meridional temperature gradients are presented as low minus high latitude mean temperatures. Crosses mark the reanalysis trends, dots mark the UKCP-PPE20 ensemble members and the squares indicate the occurrence of trends in the CMIP6 ensemble. Trends were taken over 1979-2019 for the reanalyses and UKCP-PPE20, and over 1979–2014 for CMIP6.

Overall, the observed trends are not inconsistent with simulated model trends, but are near the edge of the distribution of these in several cases, and often outside the range of the UKCP-PPE20 ensemble. Hence, the relationship between tropical warming and jet shifts requires further investigation and close monitoring in the near future.

Dynamical flux analysis. One possibility (amongst several) is that the jet streams in reality may be more sensitive to the tropical upper tropospheric warming than those in many climate models. One of the physical mechanisms thought to be important in the circulation response to localised heating is the transport of heat by atmospheric eddies[33], which then in turn leads to anomalous momentum fluxes[6,34]. Such an eddy-mediated response would be consistent with the equivalent barotropic structure in the observed wind trends. Hence, we hypothesise that the observed trends could be explained by a relatively strong increase in poleward eddy heat flux in the upper troposphere, which would act to weaken the meridional temperature gradient while simultaneously driving a strong circulation response.

Some evidence to support this hypothesis is given in Fig. 4a–d, which show the ERA5 and UKCP-PPE20 trends in eddy heat and momentum fluxes at 250 hPa. Although noisy, these show increasing trends in poleward eddy heat flux in the subtropical upper tropospheric regions of both hemispheres in ERA5, as hypothesised. They are clearest and most significant in the winter hemispheres, noting that poleward fluxes are associated with negative values in the southern hemisphere, but apparent in all cases apart from northern hemisphere summer. The magnitude of the winter fluxes (~0.5 K m s^{-1} per decade) over a spatial scale of 1000 km equates to temperature tendency trends of order 0.05 K per day per decade. Over our 40 year period, the increased heat export from the edge of the tropics is hence equivalent to a 0.2 K per day cooling, and likely an important change in the temperature budget there[35]. Similar trends in heat fluxes are also seen at 300 hPa below the jet maxima (Supplementary Fig. 4), albeit with weaker significance in some cases. This figure also
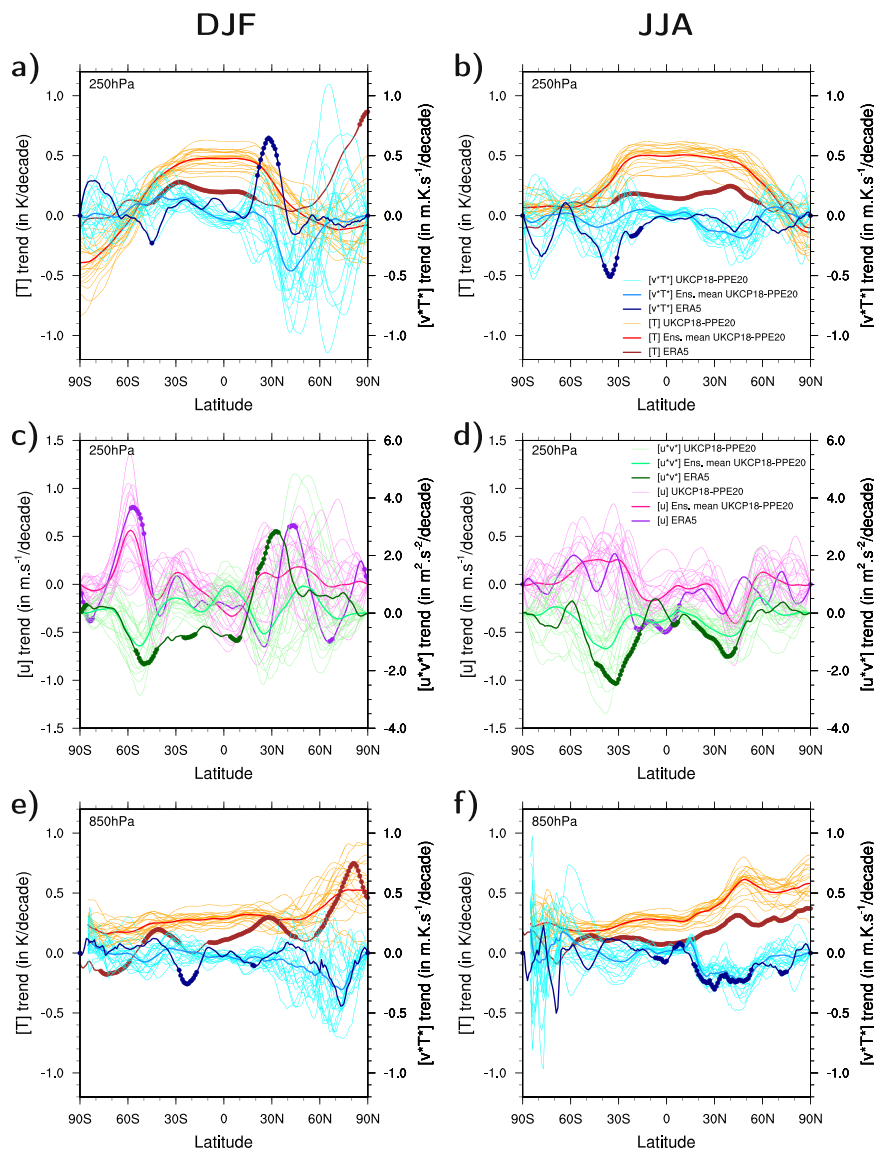

Fig. 4 Trends in poleward eddy heat and momentum fluxes (1979–2019), given by [v*T*] and [u*v*], where the brackets denote a zonal mean and the star a deviation from that. Heavy lines denote ERA5 trends, with 5% significance indicated by dots, and thin lines the trends from the UKCP-PPE20 ensemble. **a**, **b** Temperature (orange) and heat flux (blue) at 250 hPa. **c**, **d** Zonal wind (pink) and momentum fluxes (green) at 250 hPa. **e**, **f** Temperature (orange) and heat fluxes (blue) at 850 hPa. Panels (**a**, **c** and **e**) are for DJF; (**b**, **d** and **f**) are for JJA.

shows that trends in moist static energy fluxes in the upper troposphere are dominated by the trends in heat fluxes, due to the low moisture content at these altitudes.

Each region of heat flux trend is accompanied by similar trends in poleward eddy momentum flux (Fig. 4c, d), implying that the anomalous eddy activity acts to transport momentum polewards, as is common in the subtropics. The location of these trends is consistent with our hypothesis. Increased poleward eddy heat flux occurs in the subtropics, acting to extract heat from the tropical latitudes and weaken the meridional temperature gradient. Increased poleward momentum fluxes are co-located with the heat fluxes, acting to accelerate the westerlies further poleward and weaken them equatorward. These alignments are clear in both winter hemispheres and in the southern hemisphere summer. The heat and momentum fluxes are related to the vertical and meridional propagation of waves, and the changes shown here reflect a strengthening and equatorwards extension of the climatological region of upwards and equatorwards wave propagation in the subtropical upper troposphere[36]. This enhancement of wave propagation could result from the lifting of the tropopause and the associated changes in westerly winds and stability in the uppermost troposphere, as shown in Fig. 1, which will affect the propagation of waves through this region.

Although upper tropospheric heat fluxes have not been a focus of most studies, it seems that models do not typically predict such a response[7,35]. A preliminary comparison with eddy heat fluxes in models is also made in Fig. 4, using the UKCP-PPE20 ensemble. The significant observed trends are often outside the range of the model behaviour, which instead simulates a strong positive trend in meridional temperature gradient and an uncertain, but often equatorward trend in heat flux. An equatorward heat flux trend appears counterintuitive but the atmosphere does not always exhibit a flux-gradient relationship with heat fluxes directed down the temperature gradient[37]. Deeper analysis of the observed fluxes shows this not to be unusual. For example, in northern hemisphere winter the 250 hPa heat fluxes show a positive correlation with the meridional temperature gradient on decadal timescales, consistent with the observed trend, but a negative correlation on interannual timescales (Supplementary Fig. 5). This negative correlation appears to reflect the association of La Niña-like states with an anomalously cool tropical belt yet also with increased poleward eddy heat flux in this region. This arises because the Rossby waves which accomplish the heat transport are forced by enhanced surface zonal asymmetries in the tropics rather than by zonal mean warmth[37]. It is possible, therefore, that the equatorward heat flux trends in the model ensemble are associated with its more uniform pattern of tropical Pacific warming (Supplementary Fig. 6), a feature common to many models[38] and not just an artefact of the ensemble averaging shown here.

Discussion

Our hypothesis suggests that, in the context of forced climate change, the upper tropospheric eddy heat fluxes could be linked to the meridional temperature gradient through a flux-gradient relationship $[v^*T^*] = D\frac{\partial T}{\partial y}$, for some diffusivity D. The evidence presented here suggests that D may be larger in the real atmosphere than in climate models, as the observed circulation trends are relatively strong compared to the temperature gradient (Fig. 3) and feature significant heat flux trends out of the tropics, an additional process that is not represented in the model ensemble of Fig. 4. If robust, climate change in reality may be associated with a stronger meridional heat flux and a weaker temperature gradient than models predict. Consistently, the

spread in model trends in Fig. 3 is likely dominated by natural variability with no clear relationship between circulation and $\frac{\partial T}{\partial y}$. Further analysis shows the observed eddy flux trends to be dominated by seasonal and sub-seasonal timescales, with some diversity between regions, and fast variations on timescales shorter than 10 days generally make weaker contributions (Supplementary Fig. 7). Hence, these results suggest potential links between poleward jet shifts and the tropical-extratropical interactions linked to seasonal and sub-seasonal atmospheric variability[39–41]. Model fidelity in representing these interactions is one potential cause for a discrepancy in D between models and observations. Another possibility is that the observed heat fluxes are associated with natural decadal variability that is not captured by the model ensemble.

One interesting exception to many of the relationships shown here is the case of northern hemisphere summer. Observed trends show only a weak indication of a poleward jet shift and no evidence of increased upper tropospheric eddy heat fluxes. It is possible that trends in this case are driven more by a suggested weakening of synoptic-scale storm track activity[42,43]. Consistent with this, Fig. 4f shows a significant weakening of lower tropospheric eddy heat flux across most of the northern hemisphere. Interestingly, both the structure and magnitude of this trend is in close agreement with the heat flux trends in the UKCP ensemble, as are the trends in meridional temperature gradient (despite the stronger overall warming trend in the model). The reanalysis trends in moist static energy flux are again in close agreement with the heat flux trends (Supplementary Fig. 4), consistent with evidence of covarying heat and moisture fluxes over this period[44].

Another feature of interest is the weakening trend of high latitude westerlies in the northern hemisphere winter, which is potentially linked to the amplified Arctic surface warming and a weakening of the high-frequency transient eddy heat flux[45]. Models show a relationship between high latitude zonal winds and the strength of Arctic warming[9,11–13], and this relationship is reproduced in the UKCP-PPE20 ensemble. Supplementary Fig. 8 shows that stronger Arctic warming is associated with weaker zonal winds and high-frequency eddy heat fluxes in the high-latitude lower troposphere. The reanalysis trends are similar in magnitude to the stronger trends in the ensemble, highlighting the relatively strong observed warming of the Arctic. In contrast to the upper tropospheric results, however, the reanalysis points are consistent with the linear relationship in the model ensemble, suggesting that the model is capturing the response to Arctic warming well.

To summarise, there is emerging evidence that Earth's jet streams have changed significantly over the last four decades, lifting and shifting polewards. Natural variability may have played some role in this change, in addition to the effects of ozone loss in the southern hemisphere summer. However, we suggest that anthropogenic greenhouse gas emissions are also a likely driver of these trends, particularly through their effect on warming the tropical upper troposphere. Caution is of course required due to the relatively short period over which the trends are apparent, but the similarity of trends in different hemispheres/seasons is notable.

We have presented a new hypothesis that a sensitive dynamical response may contribute to the observed changes, and could have offset the increased equator-pole temperature gradient through the action of poleward eddy heat fluxes in the upper troposphere. The associated poleward eddy momentum fluxes have then contributed to the observed jet shifts. Climate models, in contrast, simulate a weaker dynamical response in which the anomalous heat is confined more to the tropics and the jet shifts are weaker. A deeper understanding of the role of upper tropospheric eddy

heat fluxes in the climate system is required, along with further testing of this hypothesis against a wider range of models and reanalyses[46].

The circulation response typically makes a significant contribution to changes in regional climate in model projections[47]. If models are indeed underestimating the sensitivity of the atmospheric circulation, as is also seen in the seasonal-decadal forecasting context[48], then projections of regional climate change could be adversely affected.

Methods

Reanalysis data. Four reanalyses were used over the period 1979 - 2019. These were ERA5[49], NCEP-NCAR[50], MERRA-2[51] and JRA-55[52].

CMIP6 model data. We used model data from the Coupled Model Intercomparison Project 6 archive (CMIP6)[53]. The data analysed here is from the historical coupled model simulations that employ prescribed external forcing (e.g. varying greenhouse gas concentrations, volcanic aerosols, anthropogenic aerosols and solar forcing). The CMIP6 historical simulations were analysed over the period that they overlap with the reanalysis datasets (1979-2014). The reanalysis trends were re-calculated over this shorter period and found to be very similar to those over the full period.

UKCP-PPE20. A 20 member Perturbed Parameter Ensemble (PPE) of global coupled simulations, 15 of which were used in the UK Climate Projections published in 2018 (UKCP18)[54]. The PPE was developed by the Met Office Hadley Centre using the HadGEM3-GC3.0.5 model, where each member only differs in the values assigned to a set of parameters[55]. Horizontal resolutions of N216 in the atmosphere and 1/4° ocean are used, with 85 and 75 vertical levels in the atmosphere and oceans respectively. This version of the HadGEM3 model precedes but is only slightly different to the version that contributes to CMIP6[55]. The resolutions are the same as those used in the seasonal forecasting configuration of the Met Office model, and are used in order to harness the improvements in regional dynamics noted in the seasonal forecast products[48].

The values of 47 parameters in the atmosphere, land surface and aerosol scheme were selected using a hierarchy of cheaper model experiments and emulation to rule out parts of parameter space that result in implausible model variants, and maximise diversity[56]. The 20-member ensemble includes the 15 members released as part of UKCP18, and five members which failed performance assessments required for use in impacts studies but remain useful for understanding model behaviour. These five show a weakening drift of their Atlantic Meridional Overturning Circulation (AMOC), and two more members showed a stronger drift in temperatures than other members. To increase the sample size, we decided to also consider these 7 members in our study as they do not show strong differences in trends over our period, in comparison with the other members (e.g. see Supplementary Fig. 8). For the comparison, daily zonal and meridional winds and temperature were used between 1979 and 2019 on three levels: 250, 500 and 850hPa. The evaluation of the ensemble at the global scale is described fully in Yamazaki et al.[55], while the design of the parameter combination for the 20 members is described in Sexton et al.[56].

Analysis. Our ERA5 analysis is based on six hourly reanalysis data from the European Centre for Medium-Range Weather Forecasts on a 1° × 1° grid. We consider winter (December to February) and summer (June to August) months for the period 1979–2019. Zonal and meridional winds and the temperature were used at different altitudes from 1000 hPa to 100 hPa. Daily averages were computed for all the data. Zonal anomalies were computed by subtracting the zonal mean from the total field. Meridional eddy fluxes of heat and momentum were calculated as $[v^*T^*]$ and $[u^*v^*]$, where u and v are the standard wind components, T is the temperature and * denotes an anomaly from the zonal mean, $[ ]$. Additionally, some fields were decomposed into high- and low-frequency parts, using a Lanczos filter with a cutoff period of 10 days, to separate the synoptic-scale variability from that of the low-frequency part[57]. Seasonal fluxes in Supplementary Fig. 7 were calculated from the seasonal mean v and T, and then subseasonal fluxes given by the total fluxes minus the seasonal and high-frequency components. The moist static energy was calculated as $c_pT + gz + Lq$ as standard, with the first two terms giving the dry static energy.

Statistics. The significance of linear trends was calculated using a two-sided T-test. The lag-1 autocorrelation of the seasonal time series in Fig. 2 was found to range from −0.08 to 0.26, and −0.14 to 0.16 if the series are detrended. None of these correlations are significant, with the correlation of 0.26 giving a p value of 0.13. Hence, no adjustment was made to account for temporal autocorrelation in the data. Note that the significance testing in Fig. 1 does not account for multiple testing, so the regions of significant trends may be overestimated. To account for this, the zonal indices used in Fig. 1 average the wind over latitude bands before

significance testing, so that multiple tests are not performed. Our assessment of the significance of the zonal mean zonal wind trends is similar to that of the IPCC AR6 report[58].

Code availability

Standard plotting tools were used and no custom code or algorithms were central to this study.

References

1. Manabe, S. & Wetherald, R. T. The effects of doubling the CO_2 concentration on the climate of a general circulation model. *J. Atmos. Sci.* **32**, 3–15 (1975).
2. Ceppi, P. & Hartmann, D. L. Connections between clouds, radiation, and midlatitude dynamics: a review. *Curr. Climate Change Rep.* **1**, 94–102 (2015).
3. Manzini, E. et al. Northern winter climate change: Assessment of uncertainty in CMIP5 projections related to stratosphere-troposphere coupling. *J. Geophys. Res.: Atmos.* **119**, 7979–7998 (2014).
4. Cohen, J. et al. Recent Arctic amplification and extreme mid-latitude weather. *Nat. Geosci.* **7**, 627–637 (2014).
5. Screen, J. A. et al. Consistency and discrepancy in the atmospheric response to arctic sea-ice loss across climate models. *Nat. Geosci.* **11**, 155–163 (2018).
6. Baker, H., Woollings, T. & Mbengue, C. Eddy-driven jet sensitivity to diabatic heating in an idealized GCM. *J. Climate* **30**, 6413–6431 (2017).
7. Lorenz, D. J. & DeWeaver, E. T. Tropopause height and zonal wind response to global warming in the IPCC scenario integrations. *J. Geophys. Res.* **112**, D10119 (2007).
8. Riviere, G. A dynamical interpretation of the poleward shift of the jet streams in global warming scenarios. *J. Atmos. Sci.* **68**, 1253–1272 (2011).
9. Harvey, B., Shaffrey, L. & Woollings, T. Equator-to-pole temperature differences and the extra-tropical storm track responses of the CMIP5 climate models. *Climate Dyn.* **43**, 1171–1182 (2014).
10. Simpson, I. R., Shaw, T. A. & Seager, R. A diagnosis of the seasonally and longitudinally varying midlatitude circulation response to global warming. *J. Atmos. Sci.* **71**, 2489–2515 (2014).
11. Zappa, G. & Shepherd, T. G. Storylines of atmospheric circulation change for European regional climate impact assessment. *J. Climate* **30**, 6561–6577 (2017).
12. Peings, Y., Cattiaux, J., Vavrus, S. J. & Magnusdottir, G. Projected squeezing of the wintertime North-Atlantic jet. *Environ. Res. Lett.* **13**, 074016 (2018).
13. Oudar, T., Cattiaux, J. & Douville, H. Drivers of the Northern extratropical eddy-driven jet change in CMIP5 and CMIP6 Models. *Geophys. Res. Lett.* **47**, e2019GL086695 (2020).
14. Mitchell, D., Thorne, P., Stott, P. & Gray, L. Revisiting the controversial issue of tropical tropospheric temperature trends. *Geophys. Res. Lett.* **40**, 2801–2806 (2013).
15. Lee, S., Gong, T., Feldstein, S. B., Screen, J. A. & Simmonds, I. Revisiting the cause of the 1989–2009 Arctic surface warming using the surface energy budget: Downward infrared radiation dominates the surface fluxes. *Geophys. Res. Lett.* **44**, 10–654 (2017).
16. Steiner, A. et al. Observed temperature changes in the troposphere and stratosphere from 1979 to 2018. *J. Climate* **33**, 8165–8194 (2020).
17. Santer, B. D. et al. Comparing tropospheric warming in climate models and satellite data. *J. Climate* **30**, 373–392 (2017).
18. Deser, C., Phillips, A., Bourdette, V. & Teng, H. Uncertainty in climate change projections: the role of internal variability. *Climate dynamics* **38**, 527–546 (2012).
19. Gillett, N. P. & Thompson, D. W. J. Simulation of recent Southern Hemisphere climate change. *Science* **302**, 273–275 (2003).

20. Archer, C. L. & Caldeira, K. Historical trends in the jet streams. *Geophys. Res. Lett.* **35**, l08803 (2008).
21. Manney, G. L. & Hegglin, M. I. Seasonal and regional variations of long-term changes in upper-tropospheric jets from reanalyses. *J. Climate* **31**, 423–448 (2018).
22. Swart, N. C., Fyfe, J. C., Gillett, N. & Marshall, G. J. Comparing trends in the southern annular mode and surface westerly jet. *J. Climate* **28**, 8840–8859 (2015).
23. Gillett, N. P., Fyfe, J. C. & Parker, D. E. Attribution of observed sea level pressure trends to greenhouse gas, aerosol, and ozone changes. *Geophys. Res. Lett.* **40**, 2302–2306 (2013).
24. Bender, F. A., Ramanathan, V. & Tselioudis, G. Changes in extratropical storm track cloudiness 1983–2008: Observational support for a poleward shift. *Climate Dyn.* **38**, 2037–2053 (2012).
25. Hoskins, B. J., James, I. N. & White, G. H. The shape, propagation and mean-flow interaction of large-scale weather systems. *J. Atmos. Sci.* **40**, 1595–1612 (1983).
26. Banerjee, A., Fyfe, J. C., Polvani, L. M., Waugh, D. & Chang, K.-L. A pause in Southern Hemisphere circulation trends due to the Montreal Protocol. *Nature* **579**, 544–548 (2020).
27. Bracegirdle, T. J., Lu, H., Eade, R. & Woollings, T. Do CMIP5 models reproduce observed low-frequency North Atlantic jet variability? *Geophys. Res. Lett.* **45**, 7204–7212 (2018).
28. Grise, K. M. et al. Recent tropical expansion: natural variability or forced response? *J. Climate* **32**, 1551–1571 (2019).
29. Lee, S. H., Williams, P. D. & Frame, T. H. Increased shear in the North Atlantic upper-level jet stream over the past four decades. *Nature* **572**, 639–642 (2019).
30. Blackport, R. & Fyfe, J. C. Climate models fail to capture strengthening wintertime North Atlantic jet and impacts on Europe. *Sci. Adv.* **8**, eabn3112 (2022).
31. Allen, R. J. & Sherwood, S. C. Warming maximum in the tropical upper troposphere deduced from thermal winds. *Nat. Geosci.* **1**, 399–403 (2008).
32. Forster, P. M., Maycock, A. C., McKenna, C. M. & Smith, C. J. Latest climate models confirm need for urgent mitigation. *Nat. Climate Change* **10**, 7–10 (2020).
33. Hwang, Y.-T. & Frierson, D. M. Increasing atmospheric poleward energy transport with global warming. *Geophys. Res. Lett.* **37** (2010).
34. Butler, A. H., Thompson, D. W. & Birner, T. Isentropic slopes, downgradient eddy fluxes, and the extratropical atmospheric circulation response to tropical tropospheric heating. *J. Atmos. Sci.* **68**, 2292–2305 (2011).
35. Wu, Y., Seager, R., Ting, M., Naik, N. & Shaw, T. A. Atmospheric circulation response to an instantaneous doubling of carbon dioxide. Part I: Model experiments and transient thermal response in the troposphere. *J. Climate* **25**, 2862–2879 (2012).
36. Edmon, H. J., Hoskins, B. J. & McIntyre, M. E. Eliassen-Palm cross sections for the troposphere. *J. Atmos. Sci.* **37**, 2600–2616 (1980).
37. Lee, S. A theory for polar amplification from a general circulation perspective. *Asia-Pacific J. Atmos. Sci.* **50**, 31–43 (2014).
38. Seager, R. et al. Strengthening tropical Pacific zonal sea surface temperature gradient consistent with rising greenhouse gases. *Nat. Climate Change* **9**, 517–522 (2019).
39. Ding, H., Greatbatch, R. J. & Gollan, G. Tropical influence independent of ENSO on the austral summer Southern Annular Mode. *Geophysical Research Letters* **41**, 3643–3648 (2014).
40. Lee, S. & Feldstein, S. B. Detecting ozone-and greenhouse gas–driven wind trends with observational data. *Science* **339**, 563–567 (2013).
41. Yoo, C., Lee, S. & Feldstein, S. B. Arctic response to an MJO-like tropical heating in an idealized GCM. *J. Atmos. Sci.* **69**, 2379–2393 (2012).
42. Coumou, D., Lehmann, J. & Beckmann, J. The weakening summer circulation in the northern hemisphere mid-latitudes. *Science* **348**, 324–327 (2015).
43. Gertler, C. G. & O'Gorman, P. A. Changing available energy for extratropical cyclones and associated convection in northern hemisphere summer. *Proceedings of the National Academy of Sciences* **116**, 4105–4110 (2019).
44. Li, M., Woollings, T., Hodges, K. & Masato, G. Extratropical cyclones in a warmer, moister climate: a recent Atlantic analogue. *Geophys. Res. Lett.* **41**, 8594–8601 (2014).
45. Chemke, R. & Polvani, L. M. Linking midlatitudes eddy heat flux trends and polar amplification. *npj Climate Atmos. Sci.* **3**, 1–8 (2020).
46. Clark, J. P., Feldstein, S. B. & Lee, S. Moist static energy transport trends in four global reanalyses: Are they downgradient? *Geophys. Res. Lett.* **49**, e2022GL098822 (2022).
47. Fereday, D., Chadwick, R., Knight, J. & Scaife, A. A. Atmospheric dynamics is the largest source of uncertainty in future winter European rainfall. *J. Climate* **31**, 963–977 (2018).
48. Scaife, A. A. & Smith, D. A signal-to-noise paradox in climate science. *npj Climate Atmos. Sci.* **1**, 1–8 (2018).
49. Hersbach, H. et al. The ERA5 global reanalysis. *Q. J. Roy. Meteorol. Soc.* **146**, 1999–2049 (2020).
50. Kalnay, E. et al. The NCEP/NCAR 40-year reanalysis project. *Bull. Amer. Meteor. Soc.* **77**, 437–471 (1996).
51. Gelaro, R. et al. The modern-era retrospective analysis for research and applications, version 2 (MERRA-2). *J. Climate* **30**, 5419–5454 (2017).
52. Kobayashi, S. et al. The JRA-55 reanalysis: general specifications and basic characteristics. *J. Meteorol. Soc. Japan. Ser. II* **93**, 5–48 (2015).
53. Eyring, V. et al. Overview of the Coupled Model Intercomparison Project Phase 6 (CMIP6) experimental design and organization. *Geosci. Model Dev.* **9**, 1937–1958 (2016).
54. Murphy, J. et al. UKCP18 land projections: Science report. Tech. Rep., UK Met Office (2018).
55. Yamazaki, K. et al. A perturbed parameter ensemble of HadGEM3-GC3.05 coupled model projections: Part 2: Global performance and future changes. *Climate Dyn.* **56**, 3437–3471 (2021).
56. Sexton, D. M. et al. A perturbed parameter ensemble of HadGEM3-GC3. 05 coupled model projections: part 1: selecting the parameter combinations. *Climate Dyn.* **56**, 3395–3436 (2021).
57. Duchon, C. E. Lanczos filtering in one and two dimensions. *J. Appl. Meteorol.* **18**, 1016–1022 (1979).
58. Gulev, S. K. et al. In *Climate Change 2021: The Physical Science Basis. Contribution of Working Group I to the Sixth Assessment Report of the Intergovernmental Panel on Climate Change*, Chap. 2 (Masson-Delmotte, V. et al.) (Cambridge University Press, 2021).

Author contributions

T.W. led the observational analysis and the writing of the paper, M.D. and C.O.R. analysed the climate model datasets, and C.M. and D.S. performed and analysed the UKCP-PPE20 experiments. All authors contributed to writing the paper.

Competing interests

The authors declare no competing interests.

Additional information

Supplementary information The online version contains supplementary material available at https://doi.org/10.1038/s43247-023-00792-8.

Correspondence and requests for materials should be addressed to Tim Woollings.

Peer review information *Communications Earth & Environment* thanks the anonymous reviewers for their contribution to the peer review of this work. Primary Handling Editors: Heike Langenberg. Peer reviewer reports are available.

Reprints and permission information is available at http://www.nature.com/reprints

Publisher's note Springer Nature remains neutral with regard to jurisdictional claims in published maps and institutional affiliations.